Soft Matter

PAPER

View Article Online
View Journal | View Issue

CrossMark click for updates

Cite this: *Soft Matter*, 2015, **11**, 5862

Toward an understanding of the thermosensitive behaviour of pH-responsive hydrogels based on cyclodextrins

Barbara Rossi,*[ab] Valentina Venuti,[c] Francesco D'Amico,[a] Alessandro Gessini,[a] Andrea Mele,[d] Carlo Punta,[d] Lucio Melone,[de] Vincenza Crupi,[c] Domenico Majolino,[c] Francesco Trotta[f] and Claudio Masciovecchio[a]

The molecular mechanism responsible for the thermosensitive behaviour exhibited by pH-responsive cyclodextrin-based hydrogels is explored here with the twofold aim of clarifying some basic aspects of H-bond interactions in hydrogel phases and contributing to a future engineering of cyclodextrin hydrogels for targeted delivery and release of bioactive agents. The degree of H-bond association of water molecules entrapped in the gel network and the extent of intermolecular interactions involving the hydrophobic/hydrophilic moieties of the polymer matrix are probed by UV Raman and IR experiments, in order to address the question of how these different and complementary aspects combine to determine the pH-dependent thermal activation exhibited by these hydrogels. Complementary vibrational spectroscopies are conveniently employed in this study with the aim of safely disentangling the spectral response arising from the two main components of the hydrogel systems, *i.e.* the polymer matrix and water solvent. The experimental evidence suggests that the dominant effects in the mechanism of solvation of cyclodextrin-based hydrogels are due to the changes occurring, upon increasing of temperature, in the hydrophobicity character of specific chemical moieties of the polymer, as triggered by pH variations. The achievements of this work corroborate the potentiality of the UV Raman scattering technique, in combination with more conventional IR experiments, to provide a "molecular view" of complex macroscopic phenomena exhibited in hydrogel phases.

Received 6th May 2015,
Accepted 15th June 2015

DOI: 10.1039/c5sm01093d

www.rsc.org/softmatter

Published on 16 June 2015. Downloaded by Politecnico di Milano on 15/07/2015 16:05:22.

Introduction

In recent years, there was a continuous effort to design and propose novel biomaterials for emerging technology problems in the medical, biological and pharmaceutical field. Hydrogels are a class of water-insoluble polymers with good swelling properties in the presence of aqueous solutions or physiological fluids, thus able to retain large fractions of water within their structure.[1,2] This class of materials appears particularly appealing for many biological and biomedical applications,[2–7] because their high water content and biocompatibility make them similar to naturally soft tissue more than any other types of biomaterials. In the last few years, the possibility to vary the chemical composition and the molecular structure of polymers allowed us to extend the use of hydrogels to tissue engineering, controlled drug delivery and bio-nanotechnology.[6,8]

More recently, extensive research focused on the design and synthesis of novel responsive hydrogel systems, *i.e.* polymer networks able to interact with their environment in a pre-programmed and intelligent manner.[9–12] Stimuli-responsive hydrogels are capable of sensing and responding to external stimuli, such as variations of temperature or pH, by varying their chemical–physical properties. For example, thermo-responsive hydrogels undergo sol–gel transitions at specific values of temperature[13–15] and they find important uses for a more targeted and convenient administration of bioactive agents, such as chemotherapeutic agents.[16] In a similar way, pH-responsive hydrogels[12,17–19] can be used as drug carriers for selective delivery of active ingredients in the intestine, where the pH value is very different from that of stomach, or incorporated within novel sensing devices.[20]

[a] *Elettra-Sincrotrone Trieste, Strada Statale 14 km 163.5, Area Science Park, 34149 Trieste, Italy. E-mail: rossi@science.unitn.it*
[b] *Department of Physics University of Trento and INSTM Local Unit, via Sommarive 14, 38123 Povo, Trento, Italy*
[c] *Department of Physics and Earth Sciences, University of Messina, Viale Ferdinando Stagno D'Alcontres 31, 98166 Messina, Italy*
[d] *Department of Chemistry, Materials and Chemical Engineering "G. Natta", Politecnico di Milano and INSTM local unit, Piazza L. da Vinci 32, Milano, 20133, Italy*
[e] *Università degli studi e-Campus, Via Isimbardi 10, 22060 Novedrate, Como, Italy*
[f] *Department of Chemistry, University of Torino, Via Pietro Giuria 7, 10125 Torino, Italy*

This journal is © The Royal Society of Chemistry 2015

Published on 16 June 2015. Downloaded by Politecnico di Milano on 15/07/2015 16:05:22.

Recently, a novel promising class of cross-linked polymers namely cyclodextrin nanosponges (NS) have been proposed by different authors as efficient platforms for sorption and delivery of both organic and inorganic species.[21–23] These polymeric materials are synthesized by the condensation reaction of the OH groups of the glucose units of cyclodextrins (CD) with suitable polyfunctional cross-linking agents (CL). The growth of the polycondensation products leads to a three-dimensional covalent network characterized by the presence of two types of cavities, namely the hydrophobic cavity of the CD units and the more hydrophilic pores of the cross-linked polymer. The peculiar porous morphology of the material has been clearly illustrated by TEM images, recently performed on samples of nanosponges.[24] NS polymers are not soluble in water, due to their extended cross-linked structure. However, they exhibit marked swelling behaviour when brought into contact with water or water solution only, affording homogeneous gel phases, as it happens for hydrogels. The formation of NS gel phases can be an efficient way to load the gel matrix with a given bioactive compound by swelling the polymer in an aqueous solution of the molecule of interest.[24]

Compared to the other types of formulations proposed as polymeric hydrogels, NS are particularly appealing due to their properties of natural and biodegradable products, as well as for their versatility.

Several examples can be found in the literature showing the performances of cyclodextrin nanosponges for uses in agriculture,[25] environmental control[26] and pharmaceutical field.[23,27,28] In particular, NS provide the advantage of an efficient tailoring of their structural and functional properties (*e.g.* hydrophobicity of chain side groups, degree of crosslinking and branches and mesh size of the gel network) by acting on specific factors during the synthesis of the polymer. Several experimental and theoretical studies consistently suggested that the most important parameters of the three-dimensional structure of NS hydrogels can be tuned by varying the chemical structure of the CL and the relative amount of CL with respect to the monomer CD (*i.e.* n = cross-linking agent in molar excess with respect to CD) used in the synthesis of NS.[29–34] Moreover, strong experimental evidence has been found that the mechanism of water uptake and the gelling behaviour of NS are intimately connected with the structural arrangement of the polymer network[35–38] as well as with the balance between hydrophobic and hydrophilic moieties in the chain side groups of the polymer.[39,40]

Based on previous spectroscopic investigations,[35] a model has been proposed for describing the swelling behaviour that leads to the formation of a NS hydrogel. When NS are brought into contact with the solvent molecules, the latter tends to progressively penetrate into the pores of nanosponges and they are retained inside the covalent polymeric network. This process is simultaneously accompanied by the non-covalent (physical) aggregation of NS domains that results in a three-dimensional network of interconnected domains extending on the macroscopic length scale (*i.e.* the gel).[35] This description of swelling phenomena of nanosponges seems to be consistent with the experimental observation[36–38] that NS hydrogels undergo the change of their physical state, from a highly viscous gel to a liquid phase, by varying the hydration level or the temperature of the system.

Recent HR-MAS NMR experiments[24] revealed that the regime of diffusivity of molecular species in NS hydrogels is modulated both by structural factors (*i.e.* the cross-linking degree of NS polymers) and by the pH variations occurring during the preparative steps affording the drug-loaded hydrogels. The latter finding suggested that the NS polymers exhibit a pH-dependent behaviour, being able to vary their water-retaining ability and their average mesh size in response to changes in environmental pH conditions.[24]

In this perspective, a full understanding of the molecular mechanisms that regulate the macroscopic responses of NS hydrogels is an essential step for the engineering of these promising biomaterials. Indeed, the explanation, at the molecular level, of the mechanism of water sorption and of the sol–gel transitions observed in NS hydrogels could be beneficial for designing a soft material to be used for optimized performances.

By exploiting the molecular sensitivity of the vibrational spectroscopy techniques, we recently studied the nature and the extent of physical interactions responsible for the complex phenomenology of hydrogels based on polymerized cyclodextrins.[35,36,39–41] The separate and complementary investigation of the molecular dynamics of the confined water and nanosponge polymer matrix[39–41] revealed that the engaged water molecules turned out to be more liquid-like and less strongly bound to the polymer's functional groups of NS.[40,41] Consequently, the gelation phenomena in NS hydrogels are thought to be driven not only by the formation of hydrogen-bond (HB) networks between water and the hydrophilic groups of polymers, but also by dispersion effects, such as the establishment of non-covalent interactions between the solvent and the more hydrophobic parts of the polymer skeleton.[39] These studies focused on the issue of how the gelling behaviour of nanosponges can be regulated by varying two important parameters, namely the hydration level and the molar ratio n.

Starting from these previous encouraging results, we are interested here to investigate the effect of pH variations on the thermosensitive response of PMA-nanosponge (PMA-NS) hydrogels, obtained by using pyromellitic anhydride (PMA) as a cross-linking agent for polymerizing β-cyclodextrin (β-CD) (Fig. 1(a) and (b)). In this paper, the transition from the gel to liquid phase observed for NS hydrogels upon increasing temperature is monitored by following the spectral modifications occurring in the UV Raman and IR spectra of the system. Particular emphasis will be devoted to explore how the pH changes can trigger different temperature-responses in NS hydrogels. The great advantage of the experimental approach exploited in this study, as already demonstrated also for other organic molecules,[42,43] is that the line shape analysis of Raman peaks separately provides information on both hydrophobic and hydrophilic chemical groups of the system by measuring the vibrational relaxation dynamics of specific molecular probes.[39,42,43] In a complementary way, the exploration of the so-called uncoupled stretching region of water molecules,[44] well visible in the IR spectra of NS hydrated with deuterated water,[40] provides a detailed view of

Published on 16 June 2015. Downloaded by Politecnico di Milano on 15/07/2015 16:05:22.

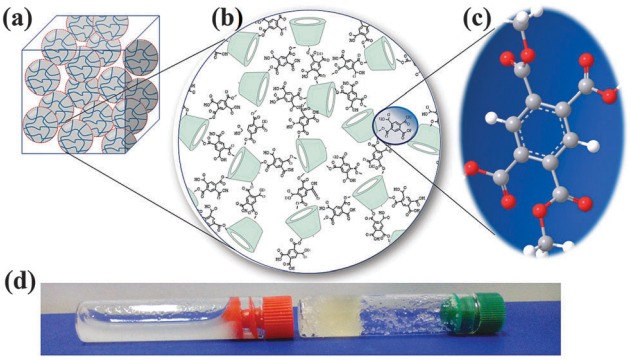

Fig. 1 Schematic illustration of (a) the network of NS hydrogels and (b) the chemical structure of PMA-NS polymers obtained by using PMA as a cross-linking agent and β-CD as a monomer. (c) Simplified model adopted for mimicking the molecular environment of the cross-linking agent PMA after the condensation with the OH groups of β-CD to form the ester bridges of the nanosponge network.[31,39,40] (d) Photographs of samples of the β-CDPMA14 hydrogel obtained by hydrating polymers with neutral H_2O (at the left) and with Na_2CO_3 solution 10% w/w (at the right) at h = 4.

the reorganization dynamics of the solvent molecules more closely confined in the pores of NS hydrogels. Overall these experiments spot on (i) the perturbation of the HB water network and its reorganization dynamics around NS groups upon increasing of temperature and (ii) the changes in the hydrophobicity character of specific chemical moieties of the polymer, as triggered by pH variations. All these results allow us to establish a clear correlation between the structure and intermolecular interactions dominating in NS hydrogels and the macroscopic responses of the system. This knowledge contributes, in turn, to a future engineering of nanosponges for targeted and controlled release of bioactive agents.

Materials and methods

A. Synthesis of nanosponge and preparation of hydrogels

PMA-NS polymers were prepared by reacting β-CD, dissolved in anhydrous DMSO and in the presence of anhydrous Et_3N, with the cross-linking agent pyromellitic anhydride (PMA) at room temperature for 3 hours under intense stirring. The cross-linker PMA was added at molecular ratios 1 : 4 with respect to the monomer CD. The obtained polymer was crushed in a mortar and purified by washing with 0.2 M HCl (aq) (3 times) and deionized water (5 times) and finally dried under vacuum affording a homogeneous powder. Previous investigations showed that, by following the synthetic protocol described above, nanosponge particles with a mean diameter of less than 1 μm can be obtained.[21]

The hydrogels of NS were prepared by adding the dry polymer samples to a suitable amount of double-distilled water (Sigma) in order to obtain the desired level of hydration h = 4 (where h is defined as weight ratio water/NS). Suitable amounts of Na_2CO_3 (10, 15, 20 and 25% w/w) were added to the hydrating water solution obtaining a final measured value of pH in the gel phase corresponding to, respectively, 8.9, 9.2, 9.7 and 10.1. After this procedure, a perfectly homogeneous and transparent gel without any visible phase separation or solid particles was obtained in about one hour time.

B. UV Raman scattering measurements and data analysis

UV Raman scattering measurements were carried out at the BL10.2-IUVS beamline at the Elettra Synchrotron laboratory in Trieste by exploiting the experimental set-up described in ref. 45. The Raman spectra were excited at 266 nm and collected in a back-scattered geometry using a triple stage spectrometer (Trivista, Princeton Instruments). The experimental resolution was set to 5 cm^{-1} in order to ensure enough resolving power and count-rates. Nanosponge hydrogels were directly freshly prepared in a UV-grade quartz cell. To minimize potential photodecomposition of the gels resulting from UV radiation exposure, the sample cell was subjected to slowly continuous spinning during the running of measurements in order to vary the illuminated sample volume through the exciting radiation beam. Polarized parallel (I_{VV}) and perpendicular (I_{HV}) Raman spectra were acquired at different values of temperature ranging from 297 to 364 K. The isotropic Raman intensity has been obtained according to the relation:

$$I_{ISO} = I_{VV} - 4/3I_{HV}.$$

The fitting procedure of the isotropic profiles has been carried out through a least squares minimization procedure, following the steps described in ref. 42 to ensure the likelihood of the results. The isotropic Raman spectral lineshape can be represented by:

$$I_{ISO} = \sum_{i=1}^{N} A_i K_i\left(\omega, \omega_0^i, \langle\omega^2\rangle^i, \tau_c^i\right) + B \quad (1)$$

where B is a flat background, A_i are the scaling factors and K_i (ω, ω_0^i,$\langle\omega^2\rangle^i$,τ_c^i) are the Kubo–Anderson functions (KAF). The latter can be expressed by the following equation:

$$K_i\left(\omega, \omega_0^i, \langle\omega^2\rangle^i, \tau_c^i\right) \propto \frac{e^{\alpha_i^2}}{\alpha_i} \sum_{n=0}^{\infty} \frac{(-\alpha_i^2)}{n!} \frac{\alpha_i + \frac{n}{\alpha_i}}{\left(\alpha_i + \frac{n}{\alpha_i}\right)^2 + \frac{(\omega - \omega_0^i)^2}{\langle\omega_i^2\rangle}} \quad (2)$$

where $\langle\omega_i^2\rangle$is the variance of the frequency spread around the unperturbed frequency ω_0^i while $\alpha = (\langle\omega^2\rangle)^{1/2}\tau_c$.

The parameters α and τ_c represent, respectively, the spread in the central frequency and the characteristic decay time of a generic stochastic perturbation acting on the vibrating atoms. If these atoms are involved in hydrogen bonds, then α and τ_c are, respectively, the spread in the central frequency due to the stochastic variance of the hydrogen bond geometry and the HB lifetime.[42] In the limit $\alpha \ll 1$ (fast modulation limit) eqn (2) can be approximated by a Lorentzian function and the parameter τ_c is related to the dephasing time τ_{deph} through the relation:

$$\tau_{deph} = \frac{1}{\langle\omega^2\rangle\tau_c} \cong \frac{1}{\pi\Gamma} \quad (3)$$

where Γ is the Lorentzian linewidth.

This journal is © The Royal Society of Chemistry 2015

Published on 16 June 2015. Downloaded by Politecnico di Milano on 15/07/2015 16:05:22.

C. FTIR-ATR absorption measurements

FTIR-ATR measurements were performed in the temperature range of 297–350 K on the nanosponge hydrogels prepared by hydration of the dry polymer β-CDPMA14 with deuterated water D_2O (hydration level h = 4), following the same procedure described in the Section A. Similarly, the final pH of the hydrogels was regulated by adding suitable amounts of Na_2CO_3 (from 10 to 25% w/w, obtaining a final pH value ranging from 8.9 to 10.1) to the hydrating water solution. The gel samples were kept at room temperature for more than 12 h before the IR measurements. No significant change in the spectrum was detected after this time, indicating the full H/D-exchange between the solvent and the polymer. The IR spectra were collected in the 400–4000 cm^{-1} wavenumber range on a Bomem DA8 Fourier transform spectrometer, operating with a Globar source, in combination with a KBr beamsplitter, a DTGS/KBr detector. The samples were contained in the Golden Gate diamond ATR system, just based on the ATR technique. The spectra were recorded in a dry atmosphere, in order to avoid dirty contributions, with a resolution of 4 cm^{-1}, automatically adding 100 repetitive scans in order to obtain a good signal-to-noise ratio and high reproducibility. All the IR spectra were normalized for taking into account the effective number of absorbers. No mathematical correction (*e.g.*, smoothing) was done, and spectroscopic manipulation such as baseline adjustment and normalization were performed using the Spectracalc software package GRAMS (Galactic Industries, Salem, NH, USA).

Results

In previous studies[31,33,34] we demonstrated that the reaction of polymerization between the cross-linking agent PMA and β-CD leads to the formation of the covalent 3D network sketched in Fig. 1(a) and (b). Fig. 1(c) displays a simplified molecular model that has been successfully used[31,39,40] for mimicking the molecular environment of the cross-linking agent PMA after the condensation with the OH groups of β-CD to form the ester bridges in the structure of nanosponges.

In the polymer network of NS, the bridges connecting adjacent cyclodextrin units and the outer surface of macrocycles contribute to define slightly hydrophilic cavities. Therefore, the formation of hydrogels by hydration of NS is supposed to occur after the progressive penetration of water molecules inside the hydrophilic pores present in the nanosponge structure.[35–38]

Moreover, the presence in the polymeric structure of NS of a great number of carboxylic groups makes the water sorption steps dependent on the pH of the starting solution, leading to a change in the mesh size of the hydrogel network[2] and in a different swelling ability of the system. For example, by hydrating β-CDPMA14 with Na_2CO_3 solution of increasing concentration (from 10 to 25% w/w), an enhancement of the swelling capability with respect to neutral H_2O is clearly observed (see photographs in Fig. 1(d)). We ascribe this behavior to the deprotonation of carboxylic groups under basic conditions, which probably causes the electrostatic repulsion of negative charges in the network, favoring the swelling process.

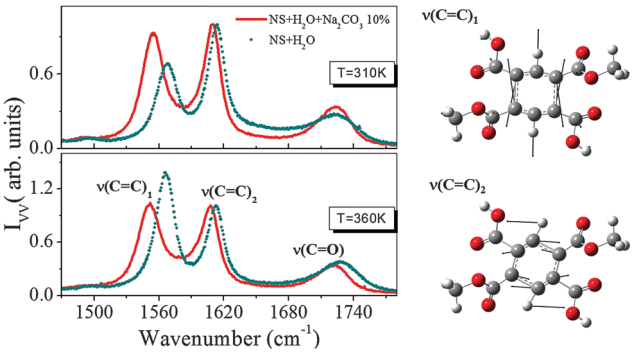

Fig. 2 Experimental UV Raman spectra of β-CDPMA14 nanosponge hydrated with H_2O (cyan symbols) and H_2O + Na_2CO_3 10% (red line) at h = 4 acquired at two different temperatures T = 310 and 360 K. Right panel: a schematic picture of the vibrational modes obtained for simulated bridging molecules,[39] labelled as ν(C=C)$_1$ and ν(C=C)$_2$.

Fig. 2 points out the comparison, at two representative values of temperature, between the Raman spectra of NS hydrogels prepared by hydrating the β-CDPMA14 polymer with pure H_2O or with 10% w/w Na_2CO_3. The acid–base interaction between solution and the polymer network is confirmed by a significant decrease of pH (8.9 measured in the hydrogel *vs.* 12.1 of the starting solution). We focused the attention on the specific wavenumber range 1500–1800 cm^{-1} reported in Fig. 2, because in this spectral window the Raman spectra of NS hydrogels are particularly informative on the water–polymer interactions established in the system, as also evidenced by recent spectroscopic measurements.[39,40]

The vibrational profiles in Fig. 2 show significant spectral modifications related to the swelling protocol used, neutral water or basic solution. A shift towards lower wavenumbers of the experimental peaks labelled as ν(C=C)$_1$ and ν(C=C)$_2$ is observed when β-CDPMA14 is hydrated with H_2O + Na_2CO_3 (red line) with respect to the case of hydration of NS with neutral water (cyan symbols). These Raman modes have been assigned to the stretching motions of the C=C bonds of the aromatic moiety of PMA[39] (Fig. 2, right panel). The changes observed in the frequency position of the vibrations ν(C=C)$_1$ and ν(C=C)$_2$ suggest that these modes are particularly sensitive to the variation of the pH of the starting hydrating solution. In particular, the ring breathing mode ν(C=C)$_1$ is observed to shift from about 1568 to 1555 cm^{-1} with increasing pH. This finding is consistent with the hypothesis that the aromatic ring CH groups of PMA tend to form C–H···O–H type intermolecular hydrogen bonds with the water molecules engaged in the hydrogel network.[39] The significant reduction of the band position revealed for ν(C=C)$_1$ in Fig. 2 suggests a strong modification of the local environment surrounding the probing oscillator upon changing the pH in the hydrogel. This fact can be, in turn, ascribed to two simultaneous effects that will be explored in depth in the following of the paper. On the one hand, (i) the C(sp^2)–H groups on PMA units are expected to show a slight acidic behaviour, *i.e.* the highly polarized CH bonds make them hydrogen bond donor sites. The C–H bond polarization is further enhanced at the basic pH value of the surrounding medium.

Published on 16 June 2015. Downloaded by Politecnico di Milano on 15/07/2015 16:05:22.

At the same time, (ii) a dynamical restructuring of the hydrogen bond network of water must be taken into account upon increasing of concentration of hydroxide ions in the solvent.

From inspection of Fig. 2, it can also be noted slight variations in the band position and shape of the vibrational signals associated with the stretching modes of the carbonyl groups of the PMA residues, generally indicated as ν(C═O). The sensitivity of this vibrational band to the pH changes seems to be enhanced at higher temperatures (Fig. 2, bottom panel), where we observe a shift towards lower wavenumbers of the mode ν(C═O) for NS hydrated with water and carbonate.

These spectral modifications reflect the ionization of the COOH pendant groups in the NS structure during the water sorption in the polymer matrix, consistently with the pH-response mechanism expected for similar hydrogel systems.[2]

Fig. 3 shows the temperature-evolution of polarized and depolarized Raman spectra of β-CDPMA14 hydrated with a solution of water and Na_2CO_3 (10% w/w) at h = 4.

All the experimental profiles were arbitrarily normalized to the intensity of the band $\nu(C{=}C)_2$, centred at about 1610 cm^{-1}, which can be assumed as a reliable internal standard, as suggested in previous Raman studies.[39]

In both polarized and depolarized Raman spectra, a marked shift towards lower wavenumbers can be clearly observed, together with an increase in intensity of the vibrational mode $\nu(C{=}C)_1$ at high T values. At the same time, only slight modifications in the frequency position of the mode $\nu(C{=}C)_2$ can be observed upon increasing T. Finally, the band associated with the stretching modes of carbonyl groups of the PMA residues does not exhibit any significant spectral change as a function of T. It is noteworthy that, as expected, the values of the depolarization ratio estimated for $\nu(C{=}C)_1$ and $\nu(C{=}C)_2$ bands remain practically constant, within the experimental error, upon increasing the temperature T (see the inset of Fig. 3).

The experimental findings of Fig. 3 once again give evidence that the CH groups on PMA residues are sensitive probes of the dynamical rearrangement of the intermolecular HB interactions that occur in the hydrogel in response to changes in T or pH.

The temperature-effects on the spectral characteristics of the mode $\nu(C{=}C)_1$ are well visible also in the isotropic Raman spectra obtained for the β-CDPMA14 hydrogel that directly reflect the pure vibrational component of the total Raman signal (Fig. 4(a)).

In order to better emphasize the temperature-evolution of isotropic profiles, we report in Fig. 4(b) the curves $I_{diff}(T)$ defined as following:

$$I_{diff}(T) = I(T) - I(T = 297\ K) \quad (4)$$

where $I(T)$ is the isotropic Raman spectrum acquired at the temperature T and $I(T = 297\ K)$ is the curve collected at T = 297 K. The difference intensities shown in Fig. 4(b) clearly evidence the raising of the spectral component centred between 1570 and 1600 cm^{-1} upon increasing temperature, besides the progressive shift towards lower wavenumbers and increasing in intensity of the mode $\nu(C{=}C)_1$ already discussed above. The appearing of a band between 1570 and 1600 cm^{-1}, not present in the spectra of NS hydrated with neutral water, could be ascribed to the establishment of intermolecular hydrogen bonds, mainly involving the CH groups of PMA. This is consistent with the modifications of the local electronic environment experienced by the aromatic moieties in the nanosponge polymeric network because of the increasing of the basicity of the solvent medium, as discussed above.

A quantitative description of the temperature-modifications described above can be achieved by the Kubo–Anderson analysis of the isotropic Raman spectra, already successfully applied to water–organic mixtures[42,43,46] and nanosponge hydrogels.[39]

Fig. 5 displays the results of the best-fitting procedure (for details see Section B of Materials and methods) of the isotropic Raman spectra of β-CDPMA14 hydrated with H_2O and Na_2CO_3 (10% w/w) at h = 4 at two representative temperatures.

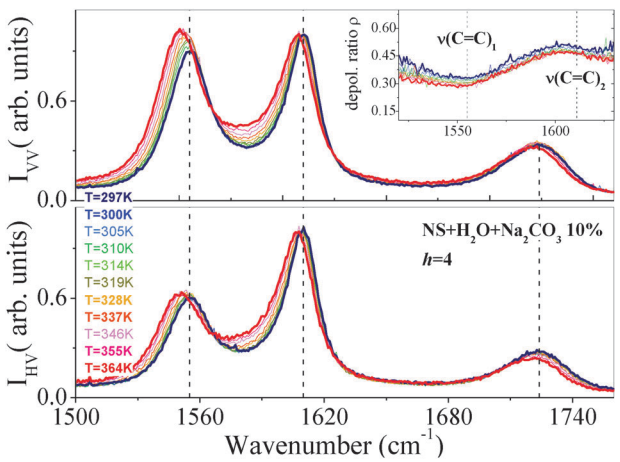

Fig. 3 Temperature-evolution of polarized I_{VV} and depolarized I_{HV} Raman intensities for β-CDPMA14 nanosponge hydrated with H_2O + Na_2CO_3 10% at h = 4. Inset: the depolarization ratio ρ reported in the wavenumber range 1520–1630 cm^{-1}.

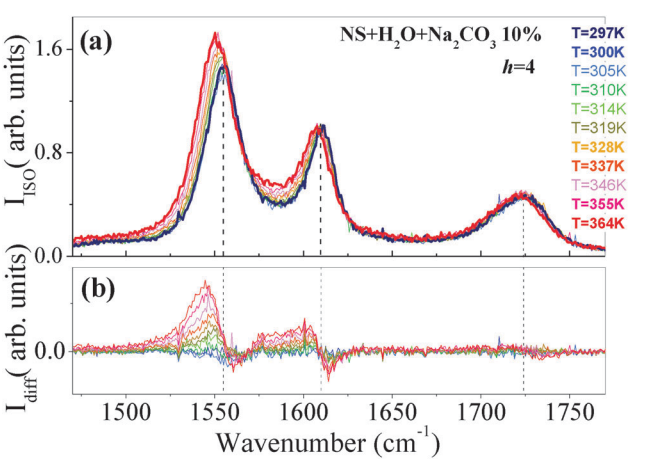

Fig. 4 (a) Temperature-evolution of isotropic Raman profiles for β-CDPMA14 nanosponge hydrated with H_2O + Na_2CO_3 10% at h = 4. (b) Difference spectral intensities I_{diff} obtained as described in the text at various temperatures T.

This journal is © The Royal Society of Chemistry 2015

Published on 16 June 2015. Downloaded by Politecnico di Milano on 15/07/2015 16:05:22.

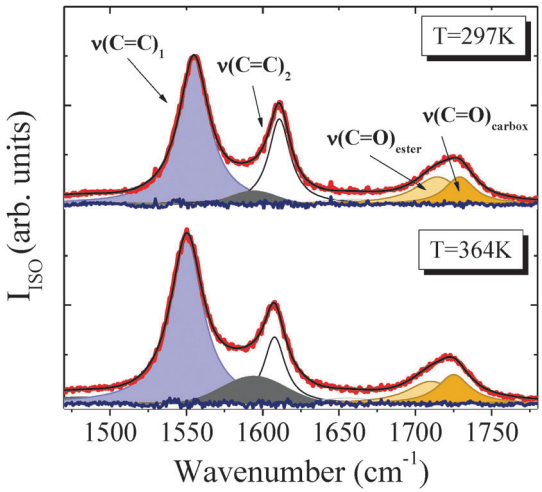

Fig. 5 Typical example of best fitting results for isotropic Raman profiles of β-CDPMA14 nanosponge hydrated with H_2O + Na_2CO_3 10% at h = 4 at two different temperatures. The total fit curve (black line) is reported together with the experimental profile (red line) and with the single components, as indicated in the panel.

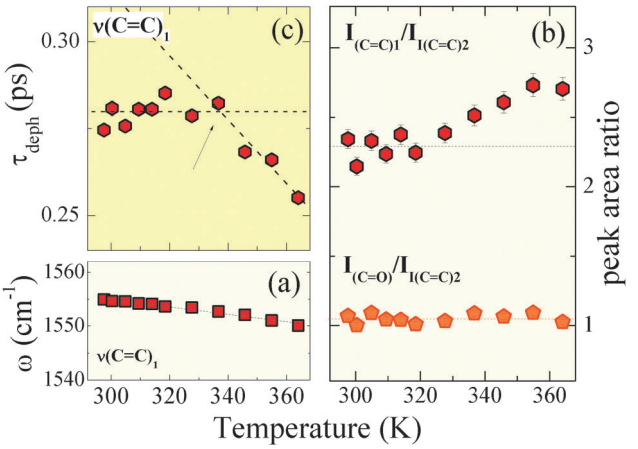

Fig. 6 Temperature-evolution of: (a) wavenumber position ω of the mode ν(C═C)$_1$ for β-CDPMA14 nanosponge hydrated with H_2O + Na_2CO_3 10% at h = 4. (b) I(C═C)$_1$/I(C═C)$_2$ and I(C═O)/I(C═C)$_2$ area ratios and (c) the dephasing time τ_{deph} associated with the ν(C═C)$_1$ Raman mode. Dotted lines are guide to eyes to highlight the T-evolutions.

The experimental profiles of Fig. 5 are well reproduced by using a total number of six KAF functions that account for the aromatic ring vibrations ν(C═C)$_1$ and ν(C═C)$_2$, while the broad band between 1570 and 1600 cm^{-1} is well represented by an additive component centred at about 1594 cm^{-1}. The asymmetric band associated with the stretching modes of the carbonyl groups of NS is modelled into two separate sub-bands, ν(C═O)$_{ester}$ and ν(C═O)$_{carbox}$, assigned to the stretching vibrations of the C═O belonging to the ester groups and to the carboxylic groups of PMA, respectively.[31,35,39,40] Finally, the contribution associated with the HOH bending mode of water (found at ~1640 cm^{-1}) was also taken into account in the total fit function, although in the spectra of hydrogels its intensity is practically negligible with respect to the signals corresponding to the vibration modes of NS.[35,39–41]

Discussion

A. Temperature-effect on hydrophobic/hydrophilic groups of polymers

Fig. 6 displays the temperature-dependence of the most significant parameters extracted from the Kubo–Anderson analysis of the vibration mode ν(C═C)$_1$ in the case of the gel sample obtained by hydrating β-CDPMA14 with H_2O and Na_2CO_3 (10% w/w) at h = 4.

As a first remark, it has to be noted that the wavenumber position of the peak corresponding to the mode ν(C═C)$_1$ linearly decreases passing from 1554 to 1550 cm^{-1} upon increasing of temperature (Fig. 6(a)). This trend may be related to the progressive enhancement of the HB interactions between the CH groups of PMA residues and the water molecules engaged in the hydrogel matrix. This behaviour is counterintuitive: indeed, the disruption, rather than the establishment, of C–H···H–O hydrogen bonds might be naively foreseen as the temperature is increased inside the gel. However, increasing the thermal motion is known to induce a destructuring effect on bulk water.[40] This, in turn, rises the population of water molecules not involved in tetrahedral structures, making a consistent quota of water molecules available for water–polymer hydrogen bonds. Thus, the reduction of the degree of hydrogen bond association in water, at the expense of the population of the solvent molecules arranged in tetrahedral HB networks,[35–38] determines a corresponding reinforcement of the dynamical perturbation induced on CH groups of PMA moieties by surrounding water, upon increasing T. This is consistently reflected by a slight increase at high T observed for the I(C═C)$_1$/I(C═C)$_2$ ratio between the peak areas corresponding to ν(C═C)$_1$ and ν(C═C)$_2$ (Fig. 6(b)).

In recent UV Raman scattering investigations performed on PMA-nanosponge hydrogels,[39] the observed increase in the polarizability of the ν(C═C)$_1$ mode has been associated with a more pronounced dynamical perturbation experienced by the CH groups of PMA due to the collision between the solvent and vibrating atoms of the polymer. Indeed, the changes in the polarizability (*i.e.* Raman activity) experimentally observed for the ν(C═C)$_1$ mode reflect the presence of surrounding water molecules that strongly perturb the vibrational dynamics of the CH groups of PMA.[39]

The panel in Fig. 6(b) points out a slight departure from the constant trend of the ratio I(C═C)$_1$/I(C═C)$_2$ starting from about T = 335 K. This suggests that for T > 335 K the CH groups in PMA moieties of the polymer network of the hydrogel are progressively more exposed to the collisions with the solvent. Conversely, the value of the ratio between the peak areas of the ν(C═O) mode and ν(C═C)$_2$ I(C═O)/I(C═C)$_2$ in Fig. 6(b) remains substantially unchanged upon increasing of temperature. This finding gives evidence that the hydrophobic groups in the chemical structure of NS are mostly sensitive to the breaking/formation of HB interactions with the solvent with respect to hydrophilic moieties.[39,40]

The analysis of the parameter α for the aromatic ring vibrations shows that, as expected, the line-shape of the peaks

Published on 16 June 2015. Downloaded by Politecnico di Milano on 15/07/2015 16:05:22.

associated with the modes $\nu(C{=}C)_1$ and $\nu(C{=}C)_2$ can be reasonably approximated by a Lorentzian function (fast modulation limit $\alpha \ll 1$). This allows us to estimate the dephasing time τ_{deph} associated with these vibration modes,[42] as described in the experimental section. The physical quantity τ_{deph} describes the time during which a molecular vibration loses the initial phase relation of its vibrational amplitude. As suggested also by other authors,[47,48] in liquid systems the inverse of τ_{deph} can be thought a reasonable estimation of the collision rate of the solvent molecules on the vibrating chemical groups. The temperature-evolution of the dephasing time τ_{deph} associated with the Raman mode $\nu(C{=}C)_1$ is shown in Fig. 6(a) for the polymer β-CDPMA14 hydrated with H_2O and Na_2CO_3 (10% w/w) at $h = 4$. The data reported in the figure clearly evidence that τ_{deph} remains substantially temperature-independent up to a value $T = T^* \cong 337$ K. For $T > T^*$ a linear decrease of the dephasing time can be observed. This trend confirms the hypothesis made above of a sudden increasing of the collision rate between water molecules and the hydrophobic CH groups on PMA moieties in NS hydrogels occurring for temperatures greater than the triggering temperature T^*.

The thermo-response observed for NS hydrogels can be interpreted, from a molecular point of view, in terms of a progressive reinforcement of the dynamical perturbation of water around the more hydrophobic parts of the NS structure, in turn resulting in a stronger solvation of the system. This finding also appears to be of particular practical interest in view of the possible applications of NS as smart thermo-responsive systems.

B. pH-dependence of the thermo-response in NS hydrogels

More interestingly, the thermo-sensitive behaviour of nanosponge hydrogels is found to be efficiently modulated by the value of pH afforded in the gel matrix during the hydration of polymers. Fig. 7 points out the temperature-dependence of the dephasing time τ_{deph} associated with the $\nu(C{=}C)_1$ Raman mode in the case of samples of β-CDPMA14 hydrogels obtained by hydrating the polymer with pure water or with aqueous solutions of Na_2CO_3.

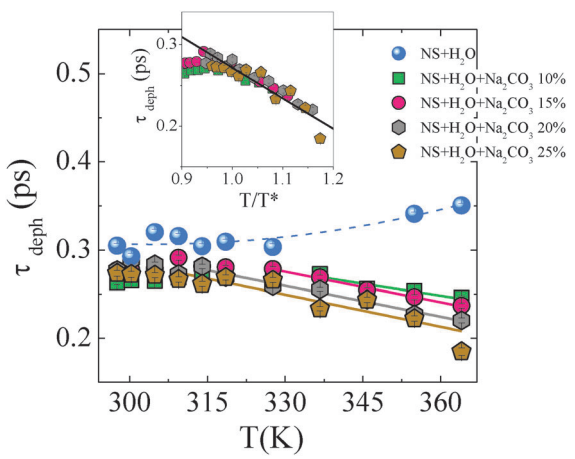

Fig. 7 Temperature-evolution of the dephasing time τ_{deph} associated with the $\nu(C{=}C)_1$ Raman mode for β-CDPMA14 nanosponge hydrated with pure H_2O (cyan symbols) and H_2O + Na_2CO_3 at 10, 15, 20 and 25% (green, pink, grey and yellow symbols, respectively) at $h = 4$. Lines are linear fit of the experimental data. Inset: dephasing time for different samples of hydrogels scaled at the estimated values of T^* (see text for details).

Table 1 Estimated values of T^* as a function of pH measured in the NS hydrogel matrix, obtained by hydrating β-CDPMA14 with aqueous solutions of Na_2CO_3 at different concentrations

w/w of Na_2CO_3 in H_2O (%)	Measured pH of gel	Estimated T^* (K)
10	8.9	337
15	9.2	328
20	9.7	314
25	10.1	310

As a first remark, it can be noted that the hydrogel prepared by using distilled water and those obtained by Na_2CO_3 solutions do exhibit opposite behaviours: τ_{deph} increases with T in the former case, while it decreases in the latter cases, with the characteristic linear relation shown in Fig. 6(c). Additionally, the T^* values determined by the plots of Fig. 7 show pH dependency. The data are summarized in Table 1. Interestingly, the values estimated for T^* are significantly lowered upon increasing the pH measured in the gel matrix, as reported in Table 1. These findings are consistent with the role played by the C–H groups as hydrogen bond donors, because of the increasing of the pH of the surrounding medium.

The accuracy of the estimation of T^* can be further confirmed by rescaling the T scale of the τ_{deph} data in terms of T/T^*, as shown in the inset of Fig. 7. It is worth noticing that, within the experimental error, the plots of τ_{deph} associated with different samples of NS hydrogels are perfectly overlapped for $T/T^* \geq 1$, collapsing into a single master curve. The existence of the master curve gives evidence that the rate of decreasing observed for τ_{deph} is essentially the same for the investigated gel samples. This result is consistent with the same thermo-response mechanism for all the NS, triggered at different critical temperatures T^* by pH variations. To explain this effect from a molecular point of view, a picture can be proposed where the basic pH value of the surrounding aqueous medium tends to enhance the slight acidic behaviour of the CH groups on the aromatic rings of PMA, in turn favouring the exposition of these hydrophobic sites to the collision with solvent molecules. Therefore, in this interpretation of the phenomena, the increasing of pH results in a corresponding increased accessibility of the polar water solvent to the hydrophobic sites of the NS polymer network and, therefore, in a thermal activation of the hydrogel response that occurs at lower temperatures.

C. Restructuring of the HB network of confined water

The counterpart of the pH-effect observed on the hydrophobic groups of the NS polymer network is given by the structural rearrangement of HB networks of water molecules localized within the pores of NS with increasing pH. The structural dynamics of confined water in different H-bonding environments can be efficiently probed by inspection of the high frequency range of the IR spectra of NS hydrated with H_2O or D_2O.[35,40]

 This journal is © The Royal Society of Chemistry 2015

Published on 16 June 2015. Downloaded by Politecnico di Milano on 15/07/2015 16:05:22.

Fig. 8 displays, as example, the IR spectrum of β-CDPMA14 hydrated with D_2O + Na_2CO_3 (10% w/w) in the wavenumber region 3000–3700 cm^{-1} where the characteristic OH stretching modes of water are typically observed.[36,38,40] As widely established by many different authors (see for example ref. 49), insights into the degree of H-bond association of bulk, interfacial and confined water is provided by the spectral analysis of the complex OH stretching band of water that can be observed in the high frequency range of Raman[37] and IR[38] spectra. By recalling a well assessed model,[50–52] the intensities of the spectral components in which the OH stretching band of water can be decomposed have been related to the different populations of H_2O molecules confined in the pores of NS polymers,[36–38] *i.e.* solvent molecules arranged in tetrahedral and non-tetrahedral HB networks. More recently, we demonstrated that more direct information on the structural rearrangement of water confined within the pores of NS are provided by applying the same spectral analysis on the so-called DHO profile.[40] By recalling what suggested by other authors in the case of hydration shell of proteins,[53] the DHO (deuterium–hydrogen–oxygen) spectrum probes the stretching modes of water molecules resulting from isotopic exchanges between the superficial H atoms of the solute and the solvent D_2O placed closely around the polymer surface. Therefore, it is reasonable to expect that the DHO spectrum reflects the spectral response arising from the population of water molecules localized in the temporarily formed hydration shells around the chemical groups of NS polymers.

The spectral profile shown in Fig. 8 for β-CDPMA14 hydrated with D_2O and Na_2CO_3 recalls the characteristic DHO profile already observed for the NS hydrogel hydrated in neutral deuterated water.[40] The DHO stretching band shown in Fig. 8 has been decomposed into the four contributions labelled as I_i (i = 1, 4) corresponding to the different populations of OH oscillators present in the system.[50–52]

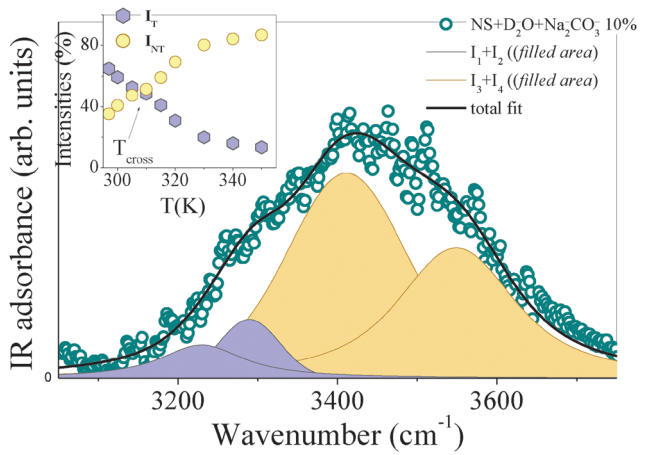

Fig. 8 Representative IR spectrum of β-CDPMA14 nanosponge hydrated with D_2O + Na_2CO_3 10% (h = 4) at T = 350 K reported in the wavenumber region 3000–3700 cm^{-1}. The experimental data (green symbols) are shown together with the typical schematic of the fitting procedure results for the DHO spectrum[40] (see the text for details). Inset: temperature evolution of $I_T = I_1 + I_2$ and $I_{NT} = I_3 + I_4$ of the spectral contributions to the DHO stretching band for β-CDPMA14 hydrated with D_2O + Na_2CO_3 10% at h = 4.

As shown in previous studies,[36–38,40] the sums of the percentage intensities of the two sub-bands found, respectively, at the lowest and highest wavenumbers, *i.e.* $(I_1 + I_2)$ and $(I_3 + I_4)$ in Fig. 8, are particularly informative of the extension of the population of water molecules arranged in tetrahedral (I_T) and non-tetrahedral (I_{NT}) HB networks.

The temperature-dependence of the intensities of the spectral contributions $I_T = I_1 + I_2$ and $I_{NT} = I_3 + I_4$ reported in the inset of Fig. 8 points out a progressive increasing of the population of water molecules involved in the HB network with connectivity less than four at the expense of the water molecules arranged in tetrahedral HB networks, upon increasing of temperature. This destructuring effect can be explained by taking into account that the increasing of thermal motion tends to break the tetrahedral arrangements of water molecules favouring the re-organization of confined water in not fully HB patterns. The trend in the inset of Fig. 8 shows, as expected,[40] the existence of a characteristic value of crossover temperature, $T_{cross} \approx 307$ K, corresponding to the temperature above which the extension of non-tetrahedral HB arrangements exceeds the population of tetrahedrally bonded water molecules. Interestingly, T_{cross} estimated for NS hydrated with water and carbonate is found to be significantly higher with respect to the cross-over point observed in the case of NS hydrated with neutral water (T = 280 K, as reported in ref. 40).

This experimental evidence suggests that the extent of the temperature disruptive effect occurring on the HB network of water engaged in NS hydrogels is affected by the pH condition of the starting hydrating solution. In particular, in the polymers swollen with basic solution, the HB network established among the water molecules confined in the nano-cavities of NS tends to be less destabilized upon increasing the temperature with respect to the case of NS swollen with neutral water. It is noteworthy that this behaviour recalls the recent finding that the temperature-disruptive effect on water molecules confined in the pores of NS is triggered by the level of the cross-linking density of the nanosponge polymer.[40] Then, the shift toward high temperature values of T_{cross} observed for NS hydrated with water and carbonate can be explained by taking into account the changes in the mesh size of the hydrogel network that favour the swelling process under basic conditions with respect to hydration of NS at neutral pH.

Surprisingly, we find that the estimated value of T_{cross} substantially does not vary with increasing pH. This result suggests that the mechanism of pH-dependence in the thermo-response of NS hydrogels is dominated, form a molecular point of view, by the structural dynamics of the more hydrophobic parts of polymers that, in turn, affects the overall solvation of the system.

Conclusions

The molecular mechanism related to the thermal response of cyclodextrin-based hydrogels is investigated here by exploiting the joint use of UV Raman scattering experiments and IR adsorption measurements. Starting from the encouraging experimental

Published on 16 June 2015. Downloaded by Politecnico di Milano on 15/07/2015 16:05:22.

results obtained in our previous studies, we address in this paper the question of how the degree of H-bond association of water molecules entrapped in the gel network and the extent of intermolecular interactions involving the hydrophobic/hydrophilic moieties of the polymer matrix cooperate to determine the pH-dependent thermal activation exhibited by nanosponge hydrogels.

Complementary vibrational spectroscopies are conveniently employed in our study with the aim of safely disentangling the spectral response arising from the two main components of the hydrogel systems, *i.e.* the polymer matrix and water solvent.

The experimental results give evidence that the hydrophobic moieties in the structure of NS polymers are mostly sensitive to the breaking/formation of HB interactions with the solvent with respect to hydrophilic groups. By distinguishing between the two molecular mechanisms that could determine, in principle, the thermo-activation of NS hydrogels, the dynamics of hydrophobic moieties of the polymer skeleton is found to dominate the solvation process of the system observed at high temperatures. This is mainly due to the enhancement of the slight acidic behaviour of the CH groups on the aromatic rings in the NS polymer network that is triggered, in turn, by pH variations. The reorganization of molecular-level interactions between CH groups and surrounding water molecules is responsible for the progressive major exposition to the solvent of the more hydrophobic sites in the polymer gel upon increasing of temperature. These overall results assume a particular practical importance in view of future engineering of nanosponge hydrogels for targeted delivery and release of bioactive agents and contribute to clarify some basic aspects of H-bond interactions in hydrogel phases. Finally, the achievements of this work corroborate the potentiality of the UV Raman scattering technique, in combination with more conventional IR experiments, to provide a ''molecular view'' of complex macroscopic phenomena.

Acknowledgements

The authors gratefully acknowledge PRIN 2010-2011 NANOMED prot. 2010 FPTBSH and PRIN 2010–2011 PROxy prot. 2010PFLRJR_005.

Notes and references

1 N. A. Peppas, B. V. Slaughter and M. A. Kanzelberger, *Hydrogels, in Comprehensive Polymer Science*, ed. R. Langer and D. Tirrell, Elsevier, 2011, vol. 9.
2 N. A. Peppas, J. Z. Hilt, A. Khademhosseini and R. Langer, *Adv. Mater.*, 2006, **18**, 1345.
3 L. A. Sharpe, A. Daily, S. Horava and N. A. Peppas, *Expert Opin. Drug Delivery*, 2014, **11**, 901.
4 Y. An and J. A. Hubbell, *J. Controlled Release*, 2000, **64**, 205.
5 C. Jen, M. C. Wake and A. G. Mikos, *Biotechnol. Bioeng.*, 1996, **50**, 357.
6 M. S. Shoichet, *Macromolecules*, 2010, **43**, 581.
7 B. V. Slaughter, S. S. Khurshid, O. Z. Fisher, A. Khademhosseini and N. A. Peppas, *Adv. Mater.*, 2009, **21**, 3307.
8 R. Langer, *Adv. Mater.*, 2009, **21**, 3235.
9 N. A. Peppas, P. Bures, W. Leobandung and H. Ichikawa, *Eur. J. Pharm. Biopharm.*, 2000, **50**, 27.
10 B. Jeong, S. Kim and Y. Bae, *Adv. Drug Delivery Rev.*, 2002, **54**, 37.
11 T. Miyata, T. Uragami and K. Nakamae, *Adv. Drug Delivery Rev.*, 2002, **54**, 79.
12 N. A. Peppas and A. R. Khare, *Adv. Drug Delivery Rev.*, 1993, **11**, 1.
13 L. Klouda and A. G. Mikos, *Eur. J. Pharm. Biopharm.*, 2008, **68**, 34.
14 Y. Y. Liu, Y. H. Shao and J. Lu, *Biomaterials*, 2006, **27**, 4016.
15 Y. B. Schuetz, R. Gurny and O. Jordan, *Eur. J. Pharm. Biopharm.*, 2008, **68**, 19.
16 R. Dinarvand and A. D'Emanuele, *J. Controlled Release*, 1995, **36**, 221.
17 G. H. Chen and A. S. Hoffman, *Nature*, 1995, **373**, 49.
18 C. A. Schoener, H. N. Hutson, G. K. Fletcher and N. A. Peppas, *Ind. Eng. Chem. Res.*, 2011, **50**(22), 12556.
19 W. B. Liechty, M. Caldorera-Moore, M. A. Phillips, C. Schoener and N. A. Peppas, *J. Controlled Release*, 2011, **155**, 119.
20 D. Snelling VanBlarcom and N. A. Peppas, *Biomed. Microdevices*, 2011, **13**, 829.
21 F. Trotta, M. Zanetti and R. Cavalli, *Beilstein J. Org. Chem.*, 2012, **8**, 2091.
22 S. Subramanian, A. Singireddy, K. Krishnamoorthy and M. Rajappan, *J. Pharm. Pharm. Sci.*, 2012, **15**(1), 103.
23 S. V. Chilajwar, P. P. Pednekar, K. R. Jadhav, G. J. C. Gupta and V. J. Kadam, *Expert Opin. Drug Delivery*, 2014, **11**(1), 111.
24 M. Ferro, F. Castiglione, C. Punta, L. Melone, W. Panzeri, B. Rossi, F. Trotta and A. Mele, *Beilstein J. Org. Chem.*, 2014, **10**, 2715.
25 L. Seglie, K. Martina, M. Devacchi, C. Roggero, F. Trotta and V. Scariot, *Postharvest Biol. Technol.*, 2011, **59**, 200.
26 D. Li, M. Ma, *Clean Products and Processes*, 2000, vol. 2, p. 112.
27 M. D. Moya-Ortega, C. Alvarez-Lorenzo, A. Concheiro and T. Loftsson, *Int. J. Pharm.*, 2012, **428**, 152.
28 E. Memisoglu-Bilensoy, I. Vural, A. Bochot, J. M. Renoir, D. Duchene and A. A. Hincal, *J. Controlled Release*, 2005, **104**, 489.
29 B. Rossi, S. Caponi, F. Castiglione, S. Corezzi, A. Fontana, M. Giarola, G. Mariotto, A. Mele, C. Petrillo, F. Trotta and G. Viliani, *J. Phys. Chem. B*, 2012, **116**(17), 5323.
30 F. Castiglione, V. Crupi, D. Majolino, A. Mele, B. Rossi, F. Trotta and V. Venuti, *J. Phys. Chem. B*, 2012, **116**(43), 13133.
31 F. Castiglione, V. Crupi, D. Majolino, A. Mele, B. Rossi, F. Trotta and V. Venuti, *J. Phys. Chem. B*, 2012, **116**(27), 7952.
32 V. Crupi, A. Fontana, M. Giarola, D. Majolino, G. Mariotto, A. Mele, L. Melone, C. Punta, B. Rossi, F. Trotta and V. Venuti, *J. Raman Spectrosc.*, 2013, **44**(10), 1457.
33 V. Crupi, A. Fontana, M. Giarola, S. Longeville, D. Majolino, G. Mariotto, A. Mele, A. Paciaroni, B. Rossi, F. Trotta and V. Venuti, *J. Phys. Chem. B*, 2014, **118**(2), 624.
34 B. Rossi, V. Venuti, A. Paciaroni, A. Mele, S. Longeville, F. Natali, V. Crupi, D. Majolino and F. Trotta, *Soft Matter*, 2015, **11**, 2183.

 This journal is © The Royal Society of Chemistry 2015

Published on 16 June 2015. Downloaded by Politecnico di Milano on 15/07/2015 16:05:22.

35 V. Crupi, D. Majolino, A. Mele, B. Rossi, F. Trotta and V. Venuti, *Soft Matter*, 2013, **9**, 6457.
36 V. Crupi, D. Majolino, A. Mele, L. Melone, C. Punta, B. Rossi, F. Toraldo, F. Trotta and V. Venuti, *Soft Matter*, 2014, **10**, 2320.
37 V. Crupi, A. Fontana, D. Majolino, A. Mele, L. Melone, C. Punta, B. Rossi, F. Rossi, F. Trotta and V. Venuti, *J. Inclusion Phenom. Macrocyclic Chem.*, 2014, **80**, 9.
38 F. Castiglione, V. Crupi, D. Majolino, A. Mele, L. Melone, W. Panzeri, C. Punta, B. Rossi, F. Trotta and V. Venuti, *J. Inclusion Phenom. Macrocyclic Chem.*, 2014, **80**, 7.
39 B. Rossi, V. Venuti, F. D'Amico, A. Gessini, F. Castiglione, A. Mele, C. Punta, L. Melone, V. Crupi, D. Majolino, F. Trotta and C. Masciovecchio, *Phys. Chem. Chem. Phys.*, 2015, **17**, 963.
40 B. Rossi, V. Venuti, A. Mele, C. Punta, L. Melone, V. Crupi, D. Majolino, F. Trotta, F. D'Amico, A. Gessini and C. Masciovecchio, *J. Chem. Phys.*, 2015, **142**(1), 014901.
41 V. Venuti, B. Rossi, F. D'Amico, A. Mele, C. Punta, L. Melone, V. Crupi, D. Majolino, F. Trotta, A. Gessini and C. Masciovecchio, *Phys. Chem. Chem. Phys.*, 2015, **17**, 10274.
42 F. D'Amico, F. Bencivenga, G. Gessini, E. Principi, R. Cucini and C. Masciovecchio, *J. Phys. Chem. B*, 2012, **116**, 13219.
43 F. D'Amico, F. Bencivenga, G. Camisasca, A. Gessini, E. Principi, R. Cucini and C. Masciovecchio, *J. Chem. Phys.*, 2013, **139**, 015101.
44 G. Bellavia, L. Paccou, S. Achir, Y. Guinet, J. Siepmann and A. Hédoux, *Food Biophys.*, 2013, **8**, 170.
45 F. D'Amico, M. Saito, F. Bencivenga, M. Marsi, A. Gessini, G. Camisasca, E. Principi, R. Cucini, S. DiFonzo and A. Battistoni, *Nucl. Instrum. Methods Phys. Res., Sect. A*, 2013, **703**, 33.
46 F. D'Amico, F. Bencivenga, A. Gessini and C. Masciovecchio, *J. Phys. Chem. B*, 2010, **114**, 10628.
47 W. G. Rothschild, *J. Chem. Phys.*, 1976, **65**, 455.
48 L. Mariani, A. Morresi, R. S. Cataliotti and M. G. Giorgini, *J. Chem. Phys.*, 1996, **104**, 914.
49 G. E. J. Walrafen, *Chem. Phys.*, 1967, **47**, 19114.
50 N. Goldman and R. J. Saykally, *J. Chem. Phys.*, 2004, **120**, 4777.
51 M. Freda, A. Piluso, A. Santucci and P. Sassi, *Appl. Spectrosc.*, 2006, **59**, 1155.
52 D. A. Schmidt and K. Miki, *J. Phys. Chem. A*, 2007, **111**, 10119.
53 G. Bellavia, L. Paccou, S. Achir, Y. Guinet, J. Siepmann and A. Hédoux, *Food Biophys.*, 2013, **8**, 170.